Deletion of *FMR1* in Purkinje Cells Enhances Parallel Fiber LTD, Enlarges Spines, and Attenuates Cerebellar Eyelid Conditioning in Fragile X Syndrome

S.K.E. Koekkoek,[1,6] K. Yamaguchi,[3,6]
B.A. Milojkovic,[1,6] B.R. Dortland,[1,6] T.J.H. Ruigrok,[1]
R. Maex,[4] W. De Graaf,[1] A.E. Smit,[1] F. VanderWerf,[1]
C.E. Bakker,[2] R. Willemsen,[2] T. Ikeda,[3] S. Kakizawa,[3]
K. Onodera,[3] D.L. Nelson,[5] E. Mientjes,[2] M. Joosten,[2]
E. De Schutter,[4] B.A. Oostra,[2] M. Ito,[3]
and C.I. De Zeeuw[1,*]
[1]Department of Neuroscience
[2]Institute of Clinical Genetics
Erasmus MC
P.O. Box 1738
3000 DR Rotterdam
The Netherlands
[3]Laboratory for Memory and Learning and Laboratory
  for Behavior Genetics
Brain Science Institute, RIKEN,
Wako, Saitama 351-0198,
Japan
[4]Laboratory of Theoretical Neurobiology
University of Antwerp
B2610 Antwerp
Belgium
[5]Department of Molecular and Human Genetics
Baylor College of Medicine
Houston, Texas

Summary

Absence of functional FMRP causes Fragile X syndrome. Abnormalities in synaptic processes in the cerebral cortex and hippocampus contribute to cognitive deficits in Fragile X patients. So far, the potential roles of cerebellar deficits have not been investigated. Here, we demonstrate that both global and Purkinje cell-specific knockouts of *Fmr1* show deficits in classical delay eyeblink conditioning in that the percentage of conditioned responses as well as their peak amplitude and peak velocity are reduced. Purkinje cells of these mice show elongated spines and enhanced LTD induction at the parallel fiber synapses that innervate these spines. Moreover, Fragile X patients display the same cerebellar deficits in eyeblink conditioning as the mutant mice. These data indicate that a lack of FMRP leads to cerebellar deficits at both the cellular and behavioral levels and raise the possibility that cerebellar dysfunctions can contribute to motor learning deficits in Fragile X patients.

Introduction

Fragile X syndrome is the most common, known monogenic cause of mental retardation (De Vries et al., 1997; Turner et al., 1996). Clinically the syndrome is characterized by mental retardation, hyperactive behavior, attention deficits, facial abnormalities, and macro-

orchidism (Hagerman and Hagerman, 2002). The gene involved is the Fragile X mental retardation 1 gene, *FMR1*, which contains in the 5′ UTR region a polymorphic CGG repeat (Fu et al., 1991; Verkerk et al., 1991). In Fragile X patients, this repeat spans more than 200 CGG units, which, in turn, causes methylation of the promoter region of *FMR1* and thereby functionally inactivates the gene. Due to inactivation of *FMR1*, its protein, FMRP, is absent in patients, while it is normally expressed in a panneuronal fashion (Verheij et al., 1993; Bakker et al., 2000).

A mouse model for Fragile X syndrome has been created by interruption of the mouse *Fmr1* gene (The Dutch-Belgian Fragile X Consortium, 1994). This knockout mouse shows behavioral and cognitive abnormalities comparable to the symptoms found in Fragile X patients, and several of these symptoms can be linked to a dysfunction of a particular brain region. For example, their enhanced startle responses to auditory stimuli and their reduced freezing behavior in response to both contextual and conditional fear stimuli indicate a malfunction of the amygdala (Chen and Toth, 2001; Nielsen et al., 2002; Paradee et al., 1999). Similarly, the tendency of the knockout mice to show a deficiency in their ability to learn the position of a hidden escape platform in a water maze task suggests hippocampal dysfunction (D'Hooge et al., 1997; Dobkin et al., 2000). To date, a potential contribution of cerebellar dysfunctions to the deficits in Fragile X patients has not been elucidated.

The pathological cellular mechanisms that may underlie the cortical behavioral and cognitive deficits described above are probably related to dysfunctions at the level of dendritic spines and their input. The dendritic spines of pyramidal cells of both Fragile X patients and *Fmr1* knockout mice are unusually long and irregular (Comery et al., 1997; Irwin et al., 2001; Rudelli et al., 1985). Since these spines appear morphologically immature, FMRP has been suggested to be involved in spine maturation and pruning, as well as in synaptogenesis (Comery et al., 1997). Indeed, FMRP and *Fmr1* mRNA are present in spines and/or dendrites, and FMRP is translated in response to activation of the type 1 metabotropic glutamate receptors (mGluR-1) in synaptoneurosomes (Weiler et al., 1997). The function of FMRP as an inhibitor of translation of bound mRNAs in vitro, including its own mRNA and that of proteins involved in microtubule-dependent synapse growth and function, indicates that FMRP may act as a regulator of activity-dependent translation in synapses (Brown et al., 2001; Li et al., 2001; Miyashiro et al., 2003). This possibility is supported by the finding that the induction of mGluR1-dependent long-term depression (LTD) is enhanced in pyramidal cells of the hippocampus in *Fmr1* knockout mice (Huber et al., 2002). Thus, altered hippocampal LTD in Fragile X patients may interfere with normal formation and maintenance of synapses required for particular cognitive functions.

Metabotropic GluR1-dependent LTD, which appears to require rapid translation of mRNA, can also be in-

*Correspondence: c.dezeeuw@erasmusmc.nl
[6]These authors contributed equally to the present study

duced at the parallel fibers (PF) to Purkinje cell (P cell) synapses in the cerebellum (Coesmans et al., 2003; Karachot et al., 2001). Absence of FMRP in cerebellar P cells could, therefore, similarly to the consequences of its absence in the pyramidal cells in the hippocampus, cause spine abnormalities in its dendrites, alter LTD induction at its PF inputs, and elicit abnormalities in motor learning behavior that specifically depends on intact cerebellar P cells, such as associative eyeblink conditioning, (Mauk and Donegan, 1997; Kim and Thompson, 1997; Yeo and Hesslow, 1998). Moreover, because the PF inputs to P cell spines compete to some extent with the climbing fiber (CF) input to their dendrites (Ichikawa et al., 2002), absence of FMRP may also affect the normal mono CF innervation of adult P-cells. Thus, to investigate the possibility that cerebellar deficits contribute to Fragile X syndrome, we tested the cerebellar learning capabilities of global and P cell-specific *Fmr1* knockout mice as well as those of Fragile X patients using classical eyeblink conditioning procedures. In addition, we investigated whether such behavioral deficits might be correlated to morphological and/or cell physiological abnormalities of the PF and CF input to P cells.

Results

Eyeblink Conditioning Is Affected in Both Global *Fmr1* Null Mutants and Purkinje Cell-Specific *L7-Fmr1* Knockouts

To find out whether a lack of FMRP can cause deficits in cerebellar eyeblink conditioning, we first subjected global *Fmr1* null mutant mice (n = 10) and wild-type littermates (n = 9), during four paired training sessions, to a classical eyeblink conditioning task (Koekkoek et al., 2002). The percentage of conditioned responses (CRs) in the global mutants was significantly reduced at sessions T2, T3, and T4 ($p < 0.05$, Student's t tests; $p < 0.005$, MANOVA) (Figure 1A). In addition, the global mutants showed significant deficits in both the peak amplitude and peak velocity of their CRs during training sessions T3 and T4, but not during sessions T1 and T2 (for both parameters at both T3 and T4, $p < 0.05$, Student's t tests) (Figures 1B and 1C). In contrast, the latencies to the onset and peak amplitude of the CRs were not significantly affected in the global null mutant (latency to onset: 109 ± 8 ms in mutants versus 102 ± 5 ms in wild-types; $p > 0.4$, Student's t test; latency to peak amplitude: 295 ± 14 ms in mutants versus 315 ± 15 ms in wild-types; $p > 0.3$, Student's t test). After two sessions of extinction, the percentages of CRs in both wild-types and global *Fmr1* null mutants were significantly reduced (in both cases, $p < 0.01$, Student's t tests). Moreover, when the conditioned stimulus (CS) and unconditioned stimulus (US) were randomly paired, virtually no CRs were observed. Finally, to determine possible effects of a lack of FMRP on the eyeblink reflex itself, we further analyzed the kinetics of the unconditioned responses (URs). The amplitudes (0.68 ± 0.03 mm) and peak velocities (44.9 ± 2.07 mm/s) of the URs in the mutants were not significantly different from those (0.73 ± 0.03 mm and 47.3 ± 2.04, respectively) in wild-types ($p > 0.25$ for both comparisons; Student's t tests). Thus, it appears unlikely that differences in sen-

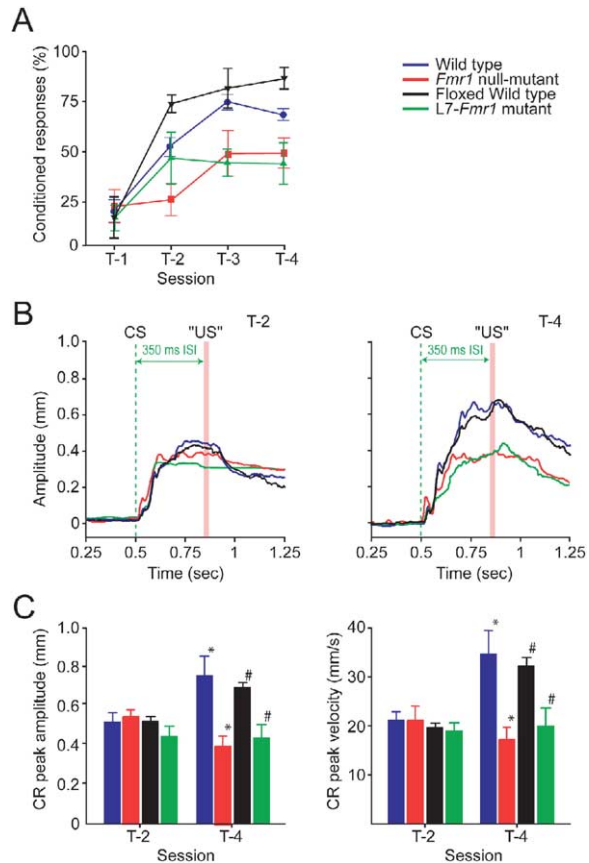
Figure 1. Eyeblink Conditioning Is Impaired in Both Global *Fmr1* Null Mutants and P Cell-Specific *L7-Fmr1* Mutants

(A) Mean percentages (± SEM) of significant CRs over 4 days of paired training for global *Fmr1* null mutants (red; n = 10) and wild-type littermates (blue; n = 9) as well as for *L7-Fmr1* mutants (green; n = 7) and floxed controls (black; n = 8). These data show that *Fmr1* mutants cannot improve the percentage of their CRs during the training as well as wild-types can. (B) Examples of data sets for training sessions T-2 (left) and T-4 (right), showing the average amplitude of CS-only responses of a representative global *Fmr1* null mutant (red), wild-type littermate (blue), *L7-Fmr1* mutant (green), and floxed control (black). Note that at T-4, both the wild-type animals and *Fmr1* mutants show reasonably well-timed responses around the moment when the US is supposed to take place ("US"), while the sizes of the responses of the *Fmr1* mutants remain fixed in amplitude over the training sessions. (C) Histograms showing average peak amplitudes and peak velocities of global *Fmr1* null mutants (red), wild-type littermates (blue), *L7-Fmr1* mutants (green), and floxed controls (black) at T-2 and T-4. In contrast to the *Fmr1* mutants, wild-type animals show a significantly increased peak amplitude and peak velocity at T-4 (for all comparisons, * $p < 0.05$ and # $p < 0.05$), but not at T-2. Error bars indicate SEM.

sitivity to the US among *Fmr1* null mutants and wild-types contribute to the differences in CRs.

Because the eyeblink paradigm in mice is largely controlled by the cerebellum (Koekkoek et al., 2003), the data described above suggest that a lack of FMRP in cerebellar neurons is at least partly responsible for the behavioral deficits. We therefore investigated to what extent the abnormal conditioning behavior can be explained by a lack of FMRP specifically in P cells, which form the main site of integration for the PF and
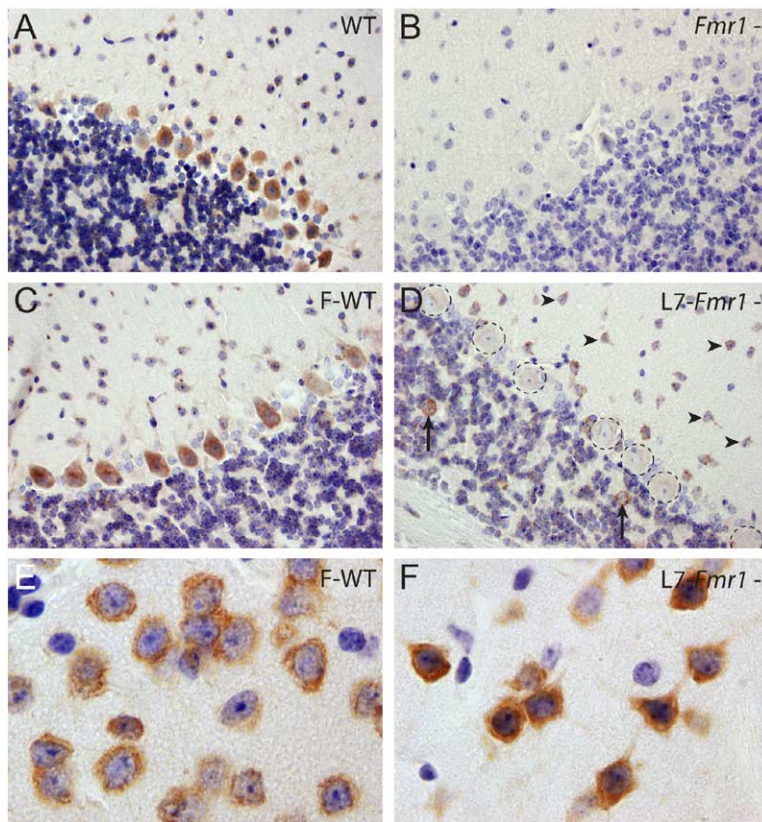
Figure 2. FMRP Expression in Wild-Type, Global *Fmr1* Null Mutant, Floxed Control, and *L7-Fmr1* Mutant Mice

FMRP expression in wild-type (A), global *Fmr1* null mutant (B), floxed control (C and E), and *L7-Fmr1* mutant (D and F) mice, using immunoperoxidase staining on paraffin sections. Note in (D) that the P cells of the *L7-Fmr1* mutant are not labeled (dashed circles), while Golgi cells (arrows) and stellate cells (arrowheads) are positively stained for FMRP in the same section. In contrast, in cerebellar sections of the global *Fmr1* null mutant (B) or the wild-types (A and C), none or all of these types of neurons are labeled, respectively. In the cerebral cortex virtually all neurons were positively labeled both in the floxed wild-type (E) and the *L7-Fmr1* mutant (F).

CF inputs and are the sole output of the cerebellar cortex. P cell-specific *Fmr1* knockout mice were created using crossbreedings of *L7-cre* mice and floxed *Fmr1* mutants. Immunohistochemical analysis demonstrated that the *L7-Fmr1* knockout mice did not express FMRP, while their surrounding neurons in the cerebellum, as well as neurons outside the cerebellum, did (Figure 2). Like the global *Fmr1* null mutants the P cell-specific *L7-Fmr1* mutants (n = 7) showed a significantly reduced percentage of CRs on days T-3 and T-4 in comparison with both the wild-type littermates of the global *Fmr1* mutants and their floxed controls (n = 8 for both sessions and both control groups; p < 0.05, Student's t tests) (Figure 1A). Moreover, the positive CRs showed significantly lower amplitudes and velocities on days T-3 and T-4 (for both parameters, p < 0.05, Student's t tests; Figures 1B and 1C), while the timing properties were unaffected (latency to onset: 115 ± 18 ms in mutants versus 111 ± 8 ms in wild-types; p > 0.7, Student's t test; latency to peak amplitude: 296 ± 17 ms in mutants versus 302 ± 17 ms in wild-types; p > 0.6, Student's t test). In addition, the amplitudes and velocities of the URs did not differ from those in their controls (p > 0.1 for all comparisons; Student's t test). These data demonstrate that a lack of FMRP in P cells alone is sufficient to replicate the deficits in eyeblink conditioning described above for the global knockout.

Startle Responses Are Enhanced in Global *Fmr1* Null Mutants but Not in Purkinje Cell-Specific *L7-Fmr1* Knockouts

Since enhanced startle responses to auditory stimuli have also been associated with Fragile X syndrome (Chen and Toth, 2001; Nielsen et al., 2002), we also analyzed the initial 60 ms periods, following the onset of the tone, of the eyeblink responses in both the global *Fmr1* mutants and P cell-specific *L7-Fmr1* mutants, as well as in their controls. This analysis showed that during all training sessions the peak amplitudes of the startle responses in the global *Fmr1* mutants, but not those in the P cell-specific *L7-Fmr1* mutants, were significantly higher than those of wild-types (for all sessions T1–T4, p < 0.001, Student's t tests) (Figure 3). Moreover, the percentage of startle responses was significantly increased during all sessions in the global *Fmr1* mutants, but not in the P cell-specific *L7-Fmr1* mutants (p < 0.05, MANOVA). These differences between the global and P cell-specific mutants suggest that a lack of FMRP in regions outside of the cerebellum can enhance the startle response, and therefore follows the notion that startle responses are controlled primarily by higher brain structures such as the amygdala (Paradee et al., 1999). In addition, these differences once again illustrate the sensitivity and specificity of the magnetic distance measurement technique (MDMT) recording method that we employ for eyeblink conditioning (Koekkoek et al., 2002; De Zeeuw et al., 2004).

LTD Is Enhanced in Purkinje Cells of both Global *Fmr1* Mutants and *L7-Fmr1* Mutants

Because deficits in eyeblink conditioning have been associated with cell physiological deficits of the PF- P cell synapse (Shibuki et al., 1996; Koekkoek et al., 2003), we investigated the induction of LTD and the efficacy of this synapse in slices of *Fmr1* mutants. LTD was in-
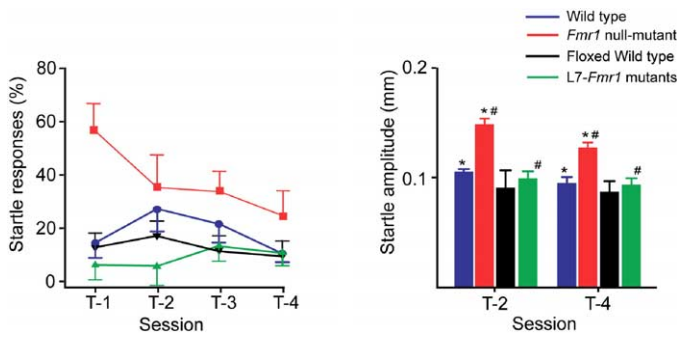
Figure 3. Startle Responses Are Enhanced in Global *Fmr1* Null Mutants, but Not in P Cell-Specific *L7-Fmr1* Mutants

(Left panel) The percentage of startle responses in wild-types and mutants during the initial 60 ms period of the eyeblink responses. Note that this percentage was significantly increased during all sessions in global *Fmr1* null mutants (red) as compared to wild-type littermates (blue), *L7-Fmr1* mutants (green), and floxed wild-type controls (black). (Right panel) Peak amplitudes of the startle responses of *Fmr1* null mutants were significantly higher than those of wild-type littermates, *L7-Fmr1* mutants, and floxed controls (p < 0.001 [* and #]; Student's t tests). Error bars indicate SEM.

duced by conjunctively applying PF stimuli and depolarizing pulses (single pulses, 140 ms duration; from −70 to +10 mV) at 1 Hz for 5 min after reaching stable recordings of EPSCs during PF stimulation at 0.2 Hz for 10 min (Miyata et al., 1999). Figure 4A shows that this conjunctive stimulation induced LTD in both wild-type (n = 7) and global *Fmr1* mutant mice (n = 6), as represented by a significant reduction in PF-EPSC (in both cases p < 0.01, Student's t tests). Hyperpolarizing pulse-evoked currents hardly changed in both wild-types and global *Fmr1* mutants (p > 0.5 in both cases, Student's t tests), implying that conjunctive stimulation does not affect access resistance, input resistance, or membrane capacitance. The change in access resis-

tance after conjunctive stimulation was no more than 2% on average in the cells used for analyses (10 wild-type and 10 mutant cells). During the 15 min period from 21 to 35 min after the onset of conjunctive stimulation, the mean amplitude of the PF-EPSCs was reduced to 70.4% ± 1.3% in wild-types and to 60.7% ± 2.3% in global *Fmr1* mutant mice. Thus, the induction of LTD in P cells of global *Fmr1* null mutants was significantly enhanced compared with that in wild-types (p < 0.01; Duncan's New Multiple Range Test) (Figure 4B). LTD was also induced using double shock stimulation of PFs at a 50 ms interval combined with the depolarizing pulse. The depression of PF-EPSC obtained with this double shock protocol in the global mutant mice was
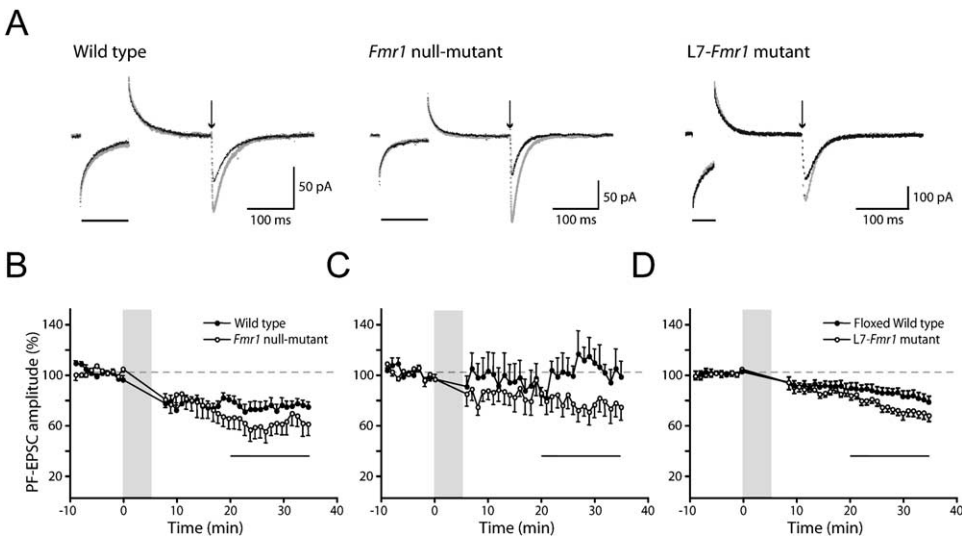

Figure 4. LTD Induction Is Enhanced in Purkinje Cells of Global *Fmr1* Null Mutants and *L7-Fmr1* Mutants

(A) Superimposed PF-EPSCs in three of the P cells recorded before conjunctive stimulation and 33 min (wild-type), 31 min (global *Fmr1* null mutant), or 32 min (*L7-Fmr1* mutants) after conjunctive stimulation, each trace representing an average of 12 traces. Note the stronger reduction of the PF-EPSCs in the mutants. Horizontal bars indicate hyperpolarizing pulses (2 mV, 100 ms) used for monitoring access resistance and input resistance, while downward arrows indicate moments of PF stimulation. (B) PF-EPSC amplitude is plotted against time before and after conjunctive stimulation averaged for 10 cells from seven wild-type mice and 10 cells from six global *Fmr1* null mutant mice. In each of these cells, 12 records successively acquired at 0.2 Hz were averaged to obtain PF-EPSC values for every minute. The shaded column indicates the period of conjunctive stimulation. (C) PF-EPSC amplitude is plotted against time for repetitive stimulation of PFs only in global *Fmr1* null mutants. (D) PF-EPSC amplitude is plotted against time before and after conjunctive stimulation averaged for seven cells from seven floxed wild-type mice and six cells from six *L7-Fmr1* mutant mice. In (B)–(D), vertical bars extending either upward or downward from the plotted points indicate SEM.

72.5% ± 1.1% (n = 5), which was relatively modest. Nevertheless, it was still enhanced compared to the depression of 81.8% ± 0.9% (n = 4) (p < 0.01, ANOVA) obtained in wild-type mice with the same double shock protocol.

To find out whether the difference in LTD induction between wild-types and global mutants is specific to conjunctive stimulation, we also tested the effect of repetitive stimulation of PFs only at 1 Hz for 5 min. Indeed, this stimulus paradigm induced depression to 75.6% ± 2.5% of the baseline values in global *Fmr1* mutants, while it did not cause a significant reduction in PF-EPSCs of P cells in wild-types. In these experiments too, the difference between wild-types and mutants was greatest 20 min after onset of the tetanus protocol. Thus, LTD induction following repetitive stimulation of PFs alone in global mutant mice is comparable to that following conjunctive stimulation in wild-type mice (p > 0.05, ANOVA), but smaller than that following conjunctive stimulation in global *Fmr1* mutants (p < 0.01, ANOVA) (Figures 4B and 4C).

The differences in LTD induction between global mutants and wild-types raise the question of whether the general synaptic efficacy of the PF-P cell synapse is also affected in *Fmr1* mutants. We therefore investigated the relationships between stimulation strength and PF-EPSC amplitude; paired-pulse facilitation of PF-EPSCs, facilitation, and fatigue of PF-EPSCs; maximum amplitude of metabotropic glutamate receptor type 1 (mGluR1)-dependent slow PF-EPSCs, thresholds, and maximum firing rate of Na^+-spikes; and maximum Ca^{2+} current and density of voltage-dependent Ca^{2+} channels in P cells. None of these parameters differed between global *Fmr1* mutants and wild-type littermates (see Table 1 in the Supplementary Data available with this article online). Thus, these control data suggest that the basic synaptic efficacy of the PF-P cell synapse is not affected in *Fmr1* mutants.

Since the PF input to the dendrites of a P cell competes with its CF input (Cesa et al., 2003; Kakizawa et al., 2000), the affected level of PF-LTD in *Fmr1* mutants may possibly be related to an abnormal CF input. We therefore investigated the strength and depression of CF-EPSCs, and we examined whether the global *Fmr1* mutants suffer from a persistent multiple CF input (Kano et al., 1998). The CF-EPSCs in mutant P cells did not show any significant anomaly in that both the absolute strength and paired-pulse depression in null mutants (n = 7) were indistinguishable from those in wild-types (n = 7) (p > 0.4 and p > 0.16, respectively, Student's t tests). The paired-pulse depression of the CF-EPSCs was 81.7% ± 1.8% in P cells of the mutant mice compared with 77.5% ± 2.3% in the wild-type mice. In regard to the number of CF inputs per P cell, we found that 60.4% of the P cells (n = 48) in wild-types tested at P21–48 showed a single-CF innervation, while double- and triple-CF innervations were observed in 35.4% and 4.2% of the cases, respectively. In mutant mice, single-, double-, and triple-CF innervations were observed in 75.6%, 22.2%, and 2.2% of the P cells (n = 45) tested, respectively. The percentage of single-CF innervation was in fact higher in the mutants than in the wild-types (p < 0.01, χ^2 test). Thus, the CF input to P cells in *Fmr1* mutants does not show any sign of a pre-

or postsynaptic deficit, and their development does not show any sign of a delay; in contrast, the normal development from multiple to mono-CF innervation is accelerated.

Finally, to investigate whether the enhancement in LTD induction is due solely to an intrinsic abnormality of P cells or whether it results from an interactive process between P cells and their surrounding neurons, we also investigated LTD of the PF-P cell synapse in cerebellar slices of the P cell-specific *L7-Fmr1* mutants. Here too, conjunctive stimulation induced LTD in both the P cell-specific *L7-Fmr1* mutant mice (n = 6) and the floxed controls (n = 7), as represented by a significant reduction in PF-EPSC (in both cases, p < 0.01, Student's t tests) (Figure 4D). Hyperpolarizing pulse-evoked currents changed minimally in both controls and mutants (p > 0.35 in both cases, Student's t tests), implying that conjunctive stimulation does not affect access resistance, input resistance, or membrane capacitance. The change in access resistance after conjunctive stimulation was no more than 3% on average in the cells used for analyses (seven control and six mutant cells). During the period from 21 to 35 min after the onset of conjunctive stimulation, the mean amplitude of the PF-EPSCs was significantly more reduced in *L7-Fmr1* mutant mice (72.9% ± 1.3%) than in controls (83.2% ± 0.8%) (p < 0.01; Duncan New Multiple Range Test). Thus, the enhancement in LTD induction found in global *Fmr1* mutants was also found in P cell-specific *L7-Fmr1* mutants, indicating that the difference with the wild-types can indeed be attributed to an intrinsic effect of the P cells themselves.

Morphology of Purkinje Cells

The finding that P cells in the cerebellum of *Fmr1* mutants show an enhanced level of LTD induction at the PF input to their dendritic spines raises the question of whether the dendritic tree of P cells in *Fmr1* mutants shows morphological abnormalities. As revealed by both calbindin immunocytochemistry and intracellular labeling with biotinylated dextran amine (BDA), the dendrites and axons of P cells of *Fmr1* null mutants appeared normal at the light microscopic level (Figure 5). The ramifications of the dendrites were not significantly different (p > 0.6, Student's t test) when analyzed with topological analyses for symmetry of arborizations (Van Pelt et al., 1992). The spine densities of distal dendrites with an average diameter smaller than 1.5 μm were 1.22 ± 0.30 spines/μm (mean ± SD) and 1.18 ± 0.27 spines/μm (mean ± SD) in *Fmr1* null mutants (n = 7) and wild-types (n = 7), respectively. Likewise, the spine density in dendritic fragments with an average diameter bigger than 1.5 μm (proximal category) was 1.26 ± 0.27 spines/μm (mean ± SD) in *Fmr1* null mutants and 1.22 ± 0.20 spines/μm (mean ± SD) in wild-types. Thus, unlike the pyramidal cells in cerebral cortical areas, the spine density of cerebellar P cells in *Fmr1* null mutants did not differ significantly from that in their wild-type littermates (distal versus distal, p > 0.5; proximal versus proximal, p > 0.5; total versus total, p > 0.5; Student's t tests).

In contrast, the shape of the spines of P cells in *Fmr1* null mutants differed from that in wild-types. Electron
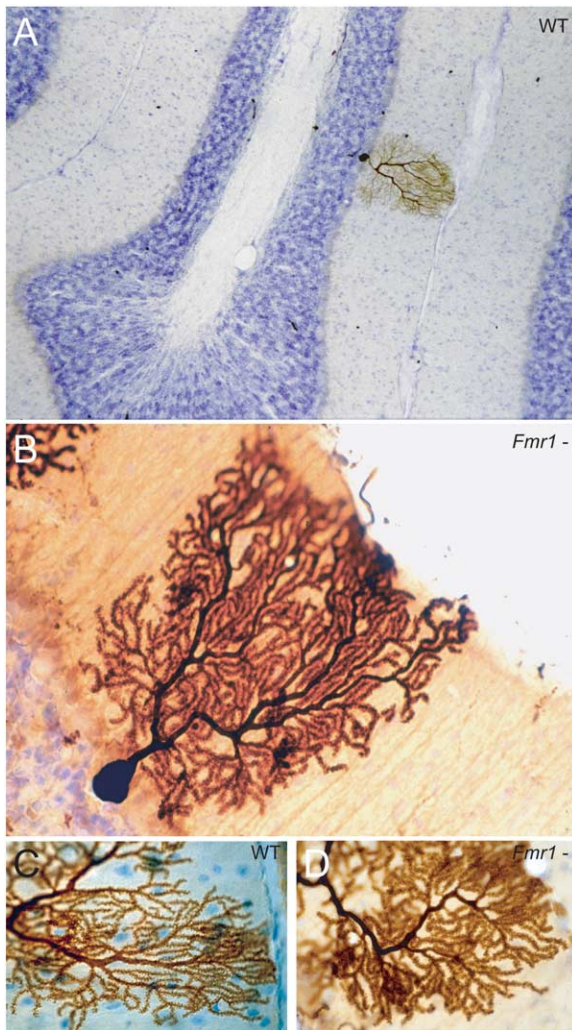
Figure 5. Dendritic Arborization of the Purkinje Cells in Global *Fmr1* Null Mutants Is Normal

Light microscopic images of the dendritic trees of P cells in wild-types (A and C) and *Fmr1* null mutants (B and D) that are retrogradely labeled with BDA. Both the topology of the P cell dendrites and the density of their spines appear normal.

microscopic analysis of calbindin-stained P cells showed that their spines were more irregular and longer (Figure 6A). The average lengths of the spine head and spine neck in *Fmr1* null mutants (0.56 ± 0.05 μm and 0.63 ± 0.18 μm, respectively; n = 4) were significantly greater than those in wild-types (0.50 ± 0.04 μm and 0.46 ± 0.15 μm, respectively; n = 4) (p < 0.05 and p < 0.001 for heads and necks, respectively; Student's t tests). The spine head diameter, spine head length/spine head diameter ratio, average spine neck diameter, and minimal spine neck diameter of *Fmr1* null mutants were not significantly different from those of wild-types (for all parameters, p > 0.2, Student's t tests). Finally, electron microscopic analyses of the spine densities did not reveal any difference, either, between mutants and wild-types (p > 0.6; Student's t test).

To find out whether the differences in lengths of spine

heads and necks were due to intrinsic changes of the P cells rather than an interaction with the environment, we also investigated the P cell spines in the *L7-Fmr1* mutant mice at the ultrastructural level (Figure 6B). The average lengths of the spine head and spine neck in *L7-Fmr1* mutants (0.57 ± 0.07 μm and 0.70 ± 0.1 μm, respectively; n = 4) were significantly greater than those in the floxed controls (0.45 ± 0.05 μm and 0.42 ± 0.08 μm, respectively; n = 4) (p < 0.05 and p < 0.02 for heads and necks, respectively; Student's t tests) (Figure 6C). No differences were observed in the densities of the spines (p > 0.4; Student's t test). Thus, similar to the global mutants, the P cell-specific *L7-Fmr1* mutants showed longer spines in which the necks were particularly elongated, while the number of spines appeared normal.

Eyeblink Conditioning Following Lesions of Cerebellar Nuclei in Trained Animals

The eyeblink data of the *Fmr1* mutants indicate that the output of the cerebellum to a large extent controls the conditioning process. However, since the mutants do not express FMRP in their P cells in early development or thereafter, we cannot exclude the possibility that secondary developmental aberrations downstream of the P cells do occur. This possibility may be especially valid for the global mutants, because the neurons involved in the eyeblink pathway downstream of the P cells also lack FMRP. We therefore investigated the change in CRs in the global *Fmr1* mutants (n = 4) and in their wild-type littermates (n = 4) after bilateral lesions of the anterior interposed nuclei, which form the ultimate cerebellar output mediating control signals for eyeblink responses (Yeo and Hesslow, 1998; Koekkoek et al., 2003). Figures 7A and 7B show an example of such lesions in an *Fmr1* mutant and their impact on the number of degenerating fibers in the superior cerebellar peduncles and the ipsilateral descending tracts, which are indicative for abundant damage in the anterior interposed nuclei (Teune et al., 2000). Following such lesions in trained wild-types and trained global *Fmr1* mutants, the percentages of CRs were reduced by 36% ± 11% and 21% ± 6%, respectively. Both changes were significant (p < 0.01 and p < 0.05, respectively; Wilcoxon rank-sum test). In addition, the remnant responses showed a reduction in amplitude (for wild-types and global *Fmr1* mutants: 42% ± 9% and 25% ± 8%, respectively) and latency to peak amplitude (for wild-types and global *Fmr1* mutants: 35% ± 1% and 30% ± 8%, respectively) (Figure 7C). Both changes were significant for both wild-types and *Fmr1* mutants (for all comparisons, p < 0.05, Wilcoxon rank-sum tests). While percentages of CRs and CR amplitude values were significantly different between wild-types and null mutants after training session T-4 before the lesion (p < 0.05 and p < 0.05, respectively; Student's t tests), these differences disappeared after the lesions (p = 0.25 and p = 0.3, respectively; Student's t tests). The results of these experiments confirm that the main differences in eyeblink conditioning parameters, such as the changes in peak amplitude and peak velocity that we observed between unlesioned *Fmr1* mutants and their wild-type littermates, are largely due to a direct
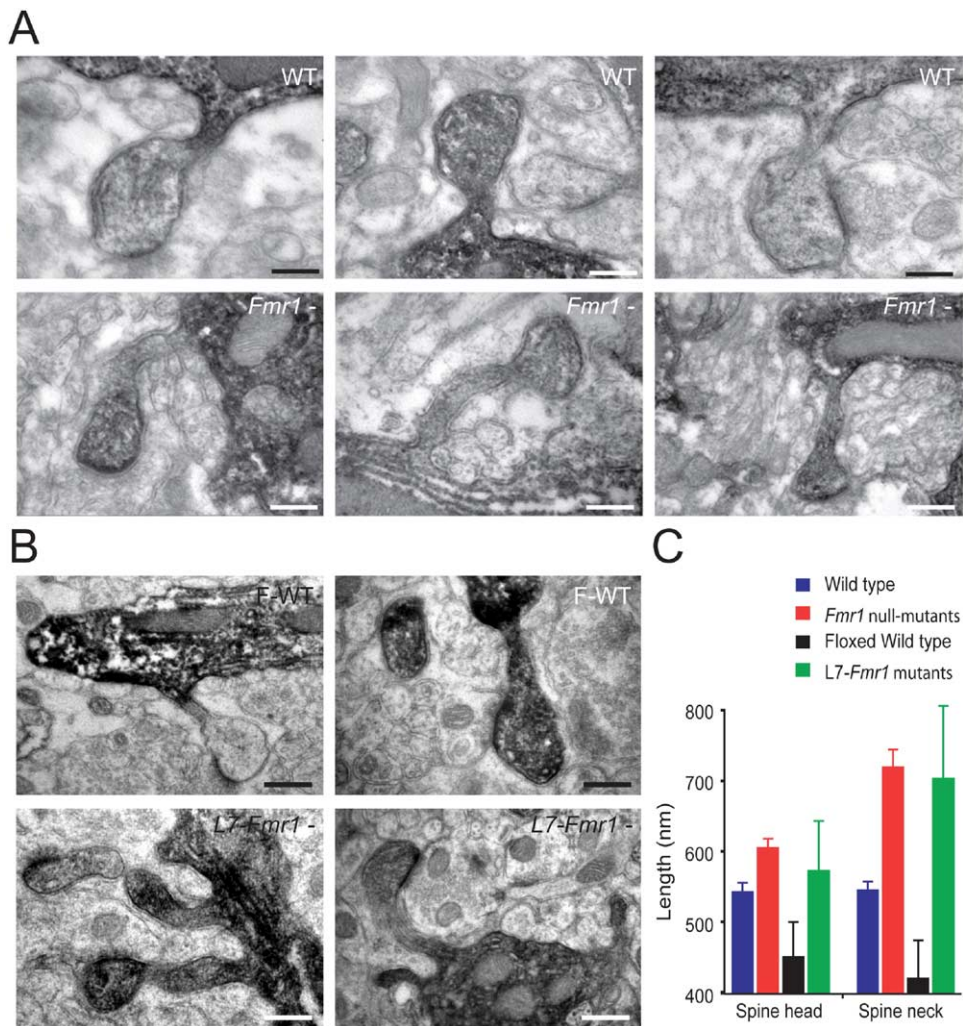
Figure 6. Ultrastructural Characteristics of Purkinje Cell Spines in *Fmr1* Null Mutants and *L7-Fmr1* Mutants Are Abnormal

(A) Electron microscopic images of the morphology of individual P cell spines in wild-types (WT; top panels) and global *Fmr1* null mutants (Fmr1–; bottom panels) that are labeled following immunocytochemistry with an antibody against calbindin. Note the longer and more irregularly shaped spines in *Fmr1* null mutants. Scale bars in micrographs of the wild-types represent 271 nm, 283 nm, and 260 nm, respectively (left to right). Scale bars in micrographs of the *Fmr1* mutants represent 297 nm, 309 nm, and 321 nm, respectively (left to right).

(B) Electron micrographs of individual P cell spines in floxed wild-types (F-WT; upper panel) and P cell-specific *L7-Fmr1* mutants (*L7-Fmr1*-; bottom panel) that are labeled following calbindin immunocytochemistry. Scale bars in micrographs of the floxed wild-types represent 279 nm and 257 nm, respectively (left to right). Scale bars in micrographs of the *L7-Fmr1* mutants represent 307 nm and 342 nm, respectively (left to right).

(C) Histograms of average lengths (+SD) of spine heads and spine necks in *Fmr1* mutants (n = 194), wild-type littermates (n = 204), *L7-Fmr1* mutants (n = 124), and floxed wild-type controls (n = 113).

difference in cerebellar control; in addition, they suggest that these differences are not due to secondary developmental aberrations downstream of their P cells.

Eyeblink Conditioning in Fragile X Patients
The data described above indicate that an animal model of Fragile X syndrome shows deficits in eyeblink conditioning and that this deficit is probably due largely to a lack of FMRP in cerebellar P cells. To find out whether a lack of functional FMRP in humans leads to the same deficits in cerebellar motor learning, we tested affected males (n = 6) and controls (n = 6), using an eyeblink conditioning task in which the eyelids are conditioned to a tone. The patients showed severe deficits (Figure 8). The peak amplitude (0.14 ± 0.03 cm) and peak velocity (3.3 ± 0.7 cm/s) in affected Fragile X males were, on average, significantly lower (p < 0.001 and p < 0.001, respectively; Student's t test) than those in normal subjects (0.54 ± 0.06 cm and 10.0 ± 1.5 cm/s, respectively). When separated according to training session (T1, T2, T3, and T4), peak amplitudes in Fragile X patients were significantly smaller than those in controls after T2, T3, and T4 (for T2 and T3, p < 0.05; for T4, p < 0.005; Student's t tests), while peak velocities in Fragile X patients were significantly smaller after T3 and T4 (in both cases, p < 0.05, Student's t tests).
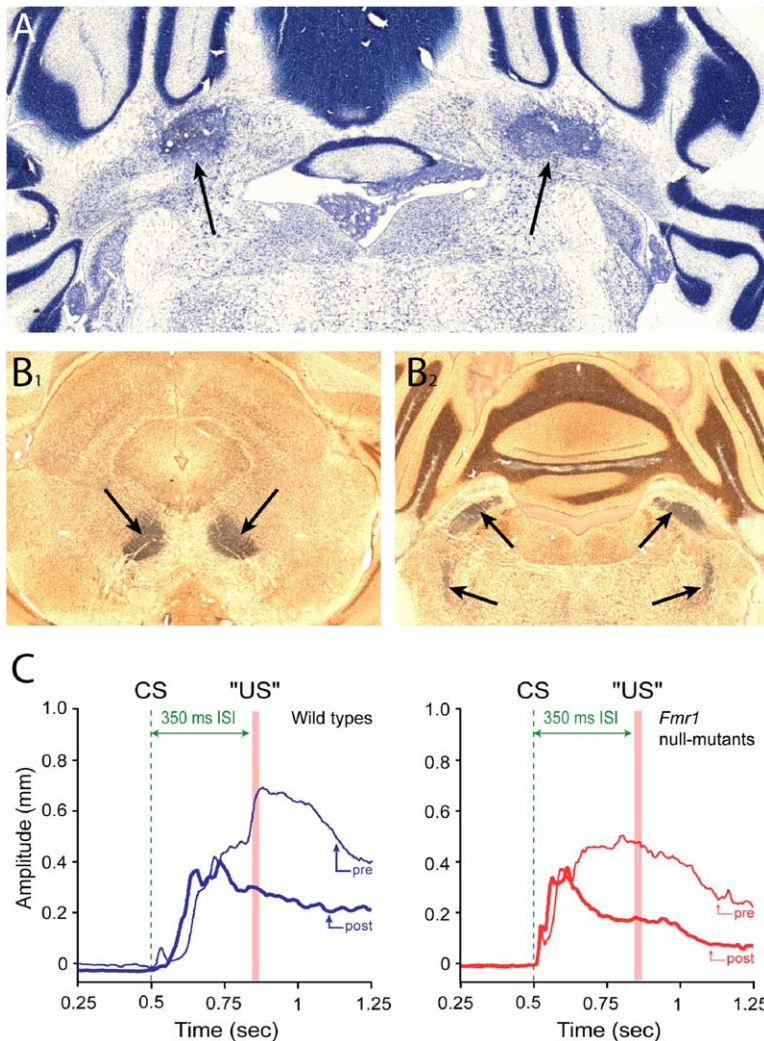
Figure 7. Bilateral Lesions of Anterior Interposed Nuclei Lead to Relatively Comparable Eyeblink Traces in Trained Wild-Types and *Fmr1* Null Mutants

(A) Example of bilateral lesion (arrows) of anterior interposed nuclei in Nissl-stained section of *Fmr1* null mutant.

(B) Example of degenerated axonal fibers (silver staining is indicated by arrows) in the superior cerebellar peduncles (left) and ipsilateral descending tracts (right); the latter are indicative for lateral damage to the anterior interposed nucleus (Teune et al., 2000).

(C) Traces showing the average amplitudes of the CRs in wild-types (left, blue) and *Fmr1* null mutants (right, red) before (thin line) and after (thick line) the lesions.

In addition, Fragile X patients showed a robust decrease in the number of CRs that were acquired during and after training (Figure 8C). The percentage of CRs was on average 80.3% ± 4.0% in control subjects and 37.6% ± 2.7% in affected males. For all sessions, the differences in the percentage of CRs were significant (T1, $p < 0.005$; T2, T3, and T4, $p < 0.001$; Student's t tests). In contrast, neither the average onset latency (0.87 ± 0.05 s) nor the average latency to peak amplitude of the CRs (0.95 ± 0.06 s) in affected males ($p = 0.29$ and $p = 0.30$, respectively; Student's t tests) differed from those in controls (0.92 ± 0.02 s and 1.02 ± 0.03 s, respectively). UR kinetics were analyzed to check for possible deficits in reflex pathways that may contribute to reduced motor learning (Figure 8C). Neither the mean amplitude (0.59 ± 0.05 cm) nor the mean velocity (13.4 ± 1.5 cm/s) of the responses in Fragile X patients differed from those in controls (0.57 ± 0.06 cm and 15.9 ± 2.0 cm/s, respectively) ($p = 0.88$ and $p = 0.31$, respectively; Student's t tests). Finally, when we subjected Fragile X patients and controls to randomly paired training paradigms, no CRs were observed. From these data, we conclude that Fragile X patients show the same deficits in eyeblink conditioning as those that we observed in the animal models of Fragile X.

Modeling Deficits in Eyeblink Conditioning Associated with Enhanced LTD

The observation that *Fmr1* mutants show both deficits in eyeblink conditioning and enhanced PF LTD raises the question of whether these two factors are causally related. Such a relationship seems counterintuitive because PF LTD is assumed to form an important memory trace for cerebellar conditioning (Koekkoek et al., 2003; Mauk and Donegan, 1997; Yeo and Hesslow, 1998). We therefore investigated whether enhanced LTD can lead to a diminished eyeblink response in a model (Figure 9). The model that we created is focused on the impact of P cells on cerebellar nuclei neurons and is based on the following assumptions: (1) during its time course, the CS activates consecutively different sets of granule cells (Medina and Mauk, 2000); (2) for each activated granule cell, the strength of LTD depends on the length of the time interval to the CF stimulus (Wang et al., 2000); (3) LTD at a PF synapse will decrease the re-
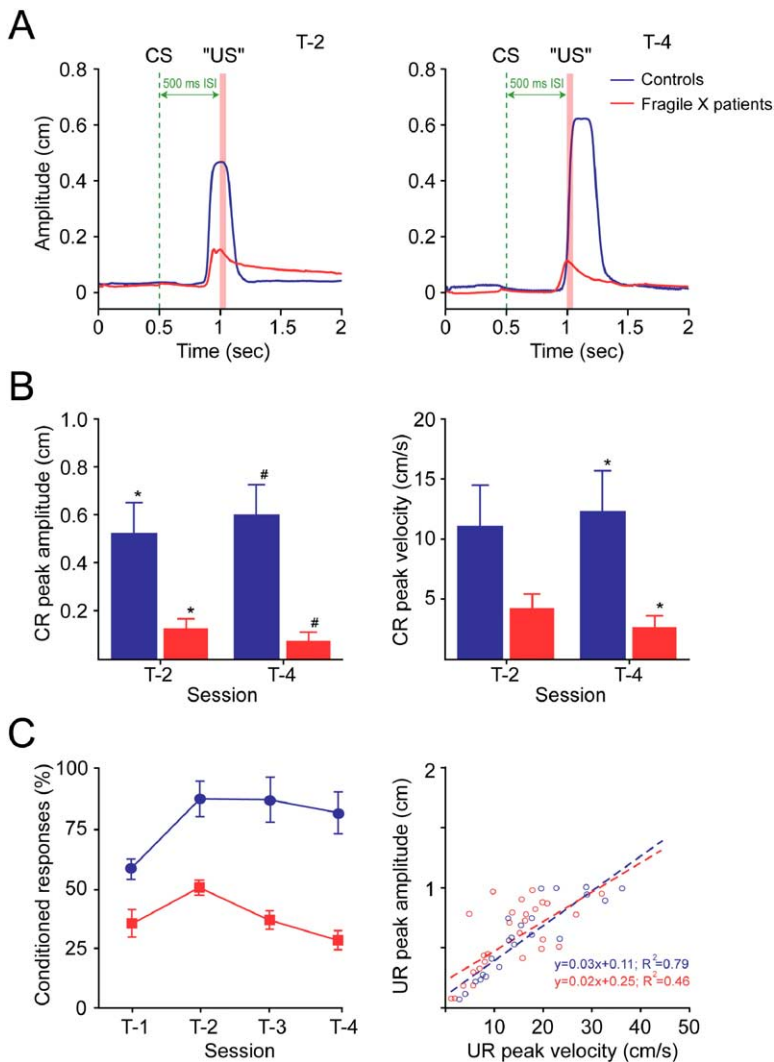
Figure 8. Eyeblink Conditioning Is Impaired in Fragile X Patients

(A) Examples of data sets for training sessions T-2 (left) and T-4 (right), showing the average amplitude of CS-only responses of a control subject (blue) and a Fragile X patient (red). (B) Histograms showing average peak amplitudes (left) and peak velocities (right) for all tested controls (n = 6) and Fragile X patients (n = 6) at T-2 and T-4. * indicates $p < 0.05$ and # indicates $p < 0.005$. (C) While the mean percentages (± SEM) of CRs in control subjects are significantly higher than those in Fragile X patients after each of the four training sessions (T1–T4; left), the kinetics of their unconditioned responses are indistinguishable from each other (right). Error bars indicate SEM.

sponse of a P cell to that PF input; (4) fast release from inhibition drives cerebellar nuclei neurons effectively through postinhibitory rebound (Aizenman and Linden, 1999, 2000); (5) the strength of the response of a cerebellar nucleus neuron will be determined not only by instantaneous changes in firing rate of the afferent P cells but also by the steady-state level of the activity of cerebellar nuclei neurons (a depolarization of the average resting membrane potential of cerebellar nuclei neurons can, by diminishing deinactivation of T-type Ca^{2+} channels, reduce the number of neurons that are available for postinhibitory rebound); (6) increased LTD in Fragile X results in reduced P cell activity and decreased inhibition of cerebellar nuclei neurons at the resting level; and (7) the motor response during a CR is determined by the instantaneous firing rate of a subpopulation of neurons in the cerebellar nuclei (Gruart et al., 1997). The details and formulas of the model are presented in the Supplementary Data (see Part II) and outlined in Figure 9. In short, the model demonstrates that a change in balance between excitation and inhibition in the cerebellar nuclei neurons, resulting from enhanced LTD at the

PF-P cell synapse, may cause a paradoxical impairment of the CR. The primary mechanism is exhaustion of the pool of cerebellar nuclei neurons capable of producing postinhibitory rebound when the CS relieves the cerebellar nuclei neurons of P cell inhibition.

Discussion

The present study shows that cerebellar abnormalities in Fragile X syndrome can occur at the morphological level, cell physiological level, and behavioral level. We found that a lack of FMRP results in a unique phenotypical combination of elongated P cell spines, enhanced LTD at the PFs that innervate these spines, and an impaired motor learning capability that is controlled by P cells. This unique combination reveals not only the extent to which cerebellar deficits may contribute to abnormalities in Fragile X syndrome but also possible clues about cerebellar function in general.

The abnormalities of dendritic spines that we observed in cerebellar P cells of both the global and cell-specific *Fmr1* null mutants mimic only partially those
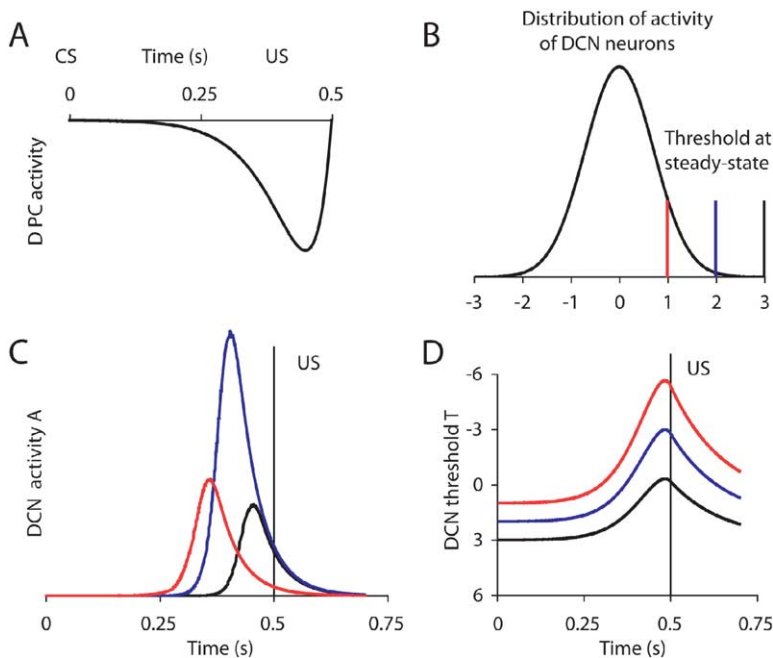
Figure 9. Mathematical Model Illustrating a Critical Sensitivity of the CR on the Steady-State Activity of P Cells (PCs) and Deep Cerebellar Nuclei (DCN) Neurons

(A) Time course of the presumed decrease in PC activity during CS presentation. This curve reflects the dependency of LTD on the relative timing of spikes in parallel and CFs during training (Wang et al., 2000).

(B) Representation of the level of excitation in the population of DCN neurons. Excitation is distributed as depicted by the standard normal curve. The blue vertical line indicates the steady-state position of the firing threshold before CS presentation; changes in PC activity cause the threshold to move leftward (disinhibition) or rightward (inhibition). Subthreshold neurons are able to produce a rebound burst when disinhibited. The leftward-shifted steady-state threshold (red line, Fragile X) indicates the increased level of excitation that enhanced LTD is predicted to produce in the cerebellar nuclei (see Kenyon et al., 1998); the black-line threshold represents the case of a decreased steady-state excitation, due to decreased LTD or intrinsic excitability.

(C) Simulated rebound DCN activity during presentation of the CS. The decrease in PC activity (depicted in [A]) drives the threshold leftward, causing disinhibited neurons to produce a rebound response. The response is clearly strongest when starting from an optimal steady state (blue curve, wild-type). Both enhanced (red curve, Fragile X) and reduced (black curve) levels of steady-state DCN excitation reduce the response amplitude.

(D) Time evolution of the threshold (upward corresponding to disinhibition) during the responses computed in (C).

that have been described for pyramidal cells in the cerebral cortex (Comery et al., 1997; Hinton et al., 1991; Irwin et al., 2002). They follow the same pattern in the morphology of individual spines appearing as immaturely shaped processes with elongated necks and heads, but they differ in that their spine density is normal. Apparently, the density of spines in P cells is more tightly regulated by compensatory mechanisms than that in pyramidal cells is. The spine density in P cells is largely subject to a well-regulated process in which the CFs and PFs compete with each other for specific sites at the dendritic tree (Cesa et al., 2003; Kakizawa et al., 2000). It is therefore attractive to hypothesize that the accelerated elimination of multiple CF inputs that we found in our electrophysiological recordings of *Fmr1* null mutants reflects a mechanism that compensates for a slowdown in spine maturation. Such a view is supported by recent data obtained by Strata and colleagues, who showed that at least two different mechanisms are responsible for spine density and spine pruning in P cells, i.e., one dependent on activity in the CFs and another one that is activity-independent (Bravin et al., 1999; Strata et al., 2000).

One of our major findings is that a lack of FMRP leads to enhanced PF LTD without affecting the basic electrical properties of P cells. Interestingly, this difference between *Fmr1* mutants and their wild-type controls, which has not been described for any other cerebellar mutant before, occurs about 15 min after the offset of conjunctive stimulation of the PFs and CFs or about 15 min after repetitive stimulation of PFs alone. This period directly follows the critical time period during which the presence and expression of one or more rapidly turned over protein(s) is/are required to induce LTD (Karachot et al., 2001). Thus, since FMRP can operate as a negative regulator of mRNA translation (Laggerbauer et al., 2001), one may assume that FMRP probably normally inhibits the translation of at least one of the proteins that is required for the expression of PF LTD 15 min after its induction. Similar time frames have been found for the impact of a lack of FMRP on the induction of LTD at the CA3-CA1 synapse in the hippocampus (Huber et al., 2002). Based on their recordings in hippocampal slices, Bear and colleagues proposed a model in which they suggest that FMRP serves to limit expression of homosynaptic LTD by inhibiting mGluR-dependent translation of local synaptic mRNAs that are involved in the stabilization of endocytosed AMPA receptors. Because PF LTD is also driven by activation of metabotropic glutamate receptors (Coesmans et al., 2003) and because PF LTD is ultimately also expressed as an endocytosis of AMPA receptors (Xia et al., 2000; Linden, 2001), their hippocampal model may also be applicable to cerebellar P cells. Considering the common specificity of the electrophysiological effects in both the hippocampus and cerebellum in that a lack of FMRP causes enhanced homosynaptic LTD without affecting basic electrophysiological properties, one would expect that the specific behavioral consequence of such a unique defect is prominently present. Unfortunately, the hippocampal deficits that can be observed in *Fmr1* null mutants subjected to spatial learning tests are partially controversial (see e.g., D'Hooge et al., 1997; Dobkin et al., 2000; Van Dam et al., 2000). Here, we show that when subjected to an associative eye-blink test, which allows us to detect deficits specific for

cerebellar motor learning, these global *Fmr1* null mutants do have a robust phenotype and that the same behavioral phenotype can be observed in P cell-specific *L7-Fmr1* mutants as well as in Fragile X patients themselves. All of them showed significantly less CRs, and they were all unable to increase the peak amplitude and peak velocity of their CRs during the training. In contrast, the latency to peak amplitude of the CRs was not significantly affected, indicating that learning-dependent timing is not severely impaired by a lack of FMRP. In this respect, the phenotype of LTD-enhanced *Fmr1* mutants diverges from that of LTD-deficient mutants. Transgenic mice in which PF LTD is selectively blocked by P cell-specific expression of an inhibitory peptide against multiple isoforms of protein kinase C (De Zeeuw et al., 1998) cannot adjust the timing of their CRs to the moment of onset of the US (Koekkoek et al., 2003). On the other hand, these LTD-deficient mice show, like the *Fmr1* mutants, a reduced percentage of CRs, and they are also unable to increase the peak amplitude and peak velocity of their CRs during the training. Thus, while the existence of PF LTD may be qualitatively necessary for the occurrence of learning-dependent timing of CRs, the exact level of PF LTD may be quantitatively responsible for the amount of CRs. Perhaps there is a level of expression of PF LTD that is optimal for attaining a maximum level of learned responses. Our model suggests that the CR may be impaired if the average level of the activity of cerebellar nuclei neurons is at a nonoptimal steady-state due to decreased inhibition by P cells. A mathematical model of cerebellar learning (Kenyon et al., 1998) predicted that enhanced LTD at the PF-P cell synapse would cause compensatory changes in the entire cerebello-olivary feedback loop. More particularly, an increased steady-state activity of cerebellar nuclei neurons would be needed to restore the balance between LTD and long-term potentiation (LTP) and to stabilize the weights of the PF-P cell synapses at nonsaturating values (see also Coesmans et al., 2004). The present model suggests that an altered steady-state level of the activity of cerebellar nuclei neurons may, in addition, impair the expression of the CR. Interestingly, the cerebellum may not be the only brain region in which an optimal rather than a maximum level of cellular plasticity is necessary for effective learning behavior. Several studies have demonstrated that a relatively mild enhancement of LTP induction in the hippocampus can be associated with impaired fear conditioning or spatial learning (Gu et al., 2002; Migaud et al., 1998).

Due to the unique aberration of enhanced LTD in *Fmr1* mutants and due to the unique combination of their deficits in classical conditioning, we have not only provided suggestive evidence for the potential importance of an optimal, instead of a maximum, level of PF LTD for cerebellar motor learning, but we have also shown that cerebellar deficits may be associated with learning deficiencies in Fragile X syndrome. Over the past decade, research on the potential roles of the cerebellum in cognitive processes has shown a remarkable advent. Investigations vary from transneuronal tracing studies, showing robust reciprocal and topographic connections between the cerebral and cerebellar cortex via the pons and thalamus (Kelly and Strick,

2003; Middleton and Strick, 1994), to clinical and neuropsychological studies, showing cognitive dysfunctions following cerebellar lesions (Leiner et al., 1993), and imaging studies, showing cerebellar activities correlated with cognitive activities (Kim et al., 1994; Vokaer et al., 2002). Thus, while a lack of FMRP in areas such as the cerebral cortex, amygdale, and hippocampus may induce cognitive symptoms in Fragile X syndrome, the current data allow us to conclude that a lack of functional FMRP in cerebellar P cells may equally well lead to deficits in motor learning in Fragile X patients.

Experimental Procedures

Eyeblink Conditioning in Mice
Wild-type and *Fmr1* mutant mice were prepared for eyeblink conditioning according to the MDMT procedure as described by Koekkoek et al. (2002). In short, mice were anesthetized, using a mixture of nitrous oxide and halothane, and a premade connector was placed on the skull. A sensor chip linked to the connector was placed over the upper eyelid, while a magnet was attached to the lower eyelid. Mice were subjected to either a paired or a randomly paired procedure in four sessions. During one session, the subject received 64 trials grouped in 8 blocks. The trials were separated by a random intertrial interval (ITI) ranging from 20 s to 40 s. In the procedure of paired training, each block consisted of one US-only trial, six paired trials, and one CS-only trial. After four sessions of paired trainings the subject was allowed to rest for 1 day, followed by two sessions of extinction. In the extinction procedure, each block consisted of one US-only trial and seven CS-only trials. In the randomly paired procedure, the US occurred randomly in the ITI, while the CS was given as described in the paired trials. In the analyses of the eyelid movements, we considered a movement as a significant eyelid response when its amplitude was greater than the mean + 3 SDs of the amplitude of the movements that occurred in the 500 ms period before the onset of the CS. Such a response was considered to contain a startle response when movement occurred within the 60 ms period directly after the onset of the CS; when significant movement occurred after this period, it was considered a CR.

Cell Physiology
Mice were anesthetized with ether and decapitated (for details, see Llano et al., 1991). The cerebellum was excised, and slices were prepared from the vermis. The recording chamber was perfused with oxygenized saline containing 100 μM picrotoxin. Recordings of P cells were obtained at 31.0°C, using an upright Nikon or Zeiss microscope, and whole-cell patch-clamp recordings were obtained with the use of borosilicate pipettes (resistance, 3–5 MΩ). Membrane current was recorded with a Multiclamp700A amplifier (Axon), while stimulation and online data acquisition were performed using pClamp 9 software (Axon). PFs and CFs were focally stimulated by applying pulses through glass pipettes positioned on the surface of the slice. Properties of voltage-gated Ca^{2+} channels in P cells were measured under voltage-clamp conditions. Slow EPSC caused by repetitive stimulation (8 pulses, 50 Hz) via type 1 metabotropic glutamate receptors (mGluR1) was measured in the presence of NBQX (10 μM) (Batchelor and Garthwaite, 1997).

Generation of Purkinje Cell-Specific *Fmr1* Knockout Mice, *L7-Fmr1* Mutant Mice
We generated conditional knockout mice in which the first coding exon of *Fmr1* can be deleted through Cre-mediated recombination. In brief, the floxed *Fmr1* allele contains a lox site 2800 bp in front of exon 1 of the *Fmr1* gene and a second lox site 260 bp after exon 1 in intron 1 of the *Fmr1* gene. Mice expressing a *L7/PCP2-cre* transgene (Barski et al. 2000) were subsequently crossed with the floxed *Fmr1* mice to generate a P cell-specific *Fmr1* knockout mouse. To confirm that FMRP was selectively not expressed in P cells, adult mice were sacrificed and processed for immunohisto-

chemical analysis of FMRP expression (for details, see Bakker et al., 2000).

Cytology of Purkinje Cells

The morphology of P cells was investigated, using BDA injections or immunocytochemistry against calbindin. BDA injections (10% in 0.1 M phosphate buffer) were made following electrophysiological identification of the cerebellar nuclei. After the iontophoretic injections, the animals were allowed to recover for 5 days and then were subsequently anesthetized (Nembutal; 50 mg/kg) and perfused with 4% paraformaldehyde in 0.1 M phosphate buffer. The brains were removed and cut in sagittal sections, which were reacted with ABC complex and diaminobenzidine to visualize the BDA. Calbindin immunocytochemistry was performed by incubating the sections with rabbit anti-calbindin antibody, ABC, and diaminobenzidine. Some of the sections were investigated under the light microscope, while others were osmicated, embedded in Durcupan, and processed for electron microscopy (De Zeeuw et al., 1989). For analysis, Purkinje cell dendrites were divided into a proximal category of dendrites (with a diameter $\geq$ 1.5 μm) and a distal category (with a diameter < 1.5 μm). Spine density was calculated by dividing the total number of spines per dendrite by the length of the dendrite. Total spine length was calculated by measuring the distance between the tip of the spine head and the base of the spine neck; spine head length was measured by multiplying the distance from the tip of the spine to the head diameter-intersection line by a factor of two; and spine neck length was calculated by subtracting the spine head length from the total spine length.

Cerebellar Lesions

The anterior interposed cerebellar nuclei were identified with the use of electrophysiological recordings in trained animals, and the lesions were subsequently made with the use of pressure injections of 200 nmol of N-methyl-D-aspartate. After recovery and new eyeblink recordings, the animals were anesthetized (Nembutal; 50 mg/kg) and transcardially perfused with 4% paraformaldehyde in 0.1 M phosphate buffer. The brains were removed and cut into sections, which were stained with silver reagents as described by Haasdijk et al. (2002).

Eyeblink Conditioning in Humans

Normal males and males with Fragile X syndrome were subjected to eyeblink conditioning procedures with the use of MDMT and video technology. MDMT as described by Koekkoek et al. (2002) was modified so it could be applied to human subjects. During MDMT recording, we simultaneously captured video frames for calibration purposes. The MDMT sensor was attached on the edge of the orbit below the right lower eyelid, while a NIB magnet was attached to the edge of the right upper eyelid. A headset containing the MDMT amplifier, MDMT power supply, puff nozzle, miniature camera, and headphones was mounted on the head of the subject. Subjects were seated before a monitor and allowed to watch a movie. The headset provided a head-free recording situation, which is necessary when dealing with mentally compromised patients. The puff nozzle was set to direct the air puff to the cornea close to the outer canthus of the eye at a distance of 15 mm. The puff had an intensity of 20 PSI at the source, while stimulus duration was set at 20 ms. The sound of the movie acted as background noise, and volume was adjusted to an average of 75 dB. The CS was a 650 Hz tone at 75 dB with a duration of 520 ms starting 500 ms prior to US delivery (interstimulus interval, 500 ms). The headset provided complete sound isolation from the environment. The training was divided into four training sessions with two blocks of eight trials each. Each block contained one CS-only and one US-only trial, which were randomly distributed. The ITI was randomly determined but always ranged from 10 s to 30 s. All data values were obtained from CS-only trials, with the exception of UR data values. In the randomly paired procedure, the US occurred randomly in the ITI, while the CS was given as in the paired trials. For analysis criteria, see Koekkoek et al. (2002).

Model

Simulations were performed with custom-written C code. Differential equations (see Supplemental Data) were integrated with the forward Euler method. In population models like the present one, there is an unavoidable lack of data to constrain all parameters. We therefore confirmed that the main finding, i.e., the critical dependence of the CR amplitude on the steady-state level of activity in P cells and neurons of the cerebellar nuclei, can be reproduced in models sharing these features: the instantaneous response of cerebellar nuclear neurons is dominated by rebound discharges, the rebound discharge depends on the level of inhibition, and the pool of neurons available for disinhibition, or the overall rebound response, can be exhausted.

Supplemental Data

Supplemental Data include a table and sections of text pertaining to cell physiology, the mathematical model used, and the results and can be found with this article online at http://www.neuron.org/cgi/content/full/47/3/339/DC1/.

References

Aizenman, C.D., and Linden, D.J. (1999). Regulation of the rebound depolarization and spontaneous firing patterns of deep nuclear neurons in slices of rat cerebellum. J. Neurophysiol. *82*, 1697–1709.

Aizenman, C.D., and Linden, D.J. (2000). Rapid, synaptically driven increases in the intrinsic excitability of cerebellar deep nuclear neurons. Nat. Neurosci. *3*, 109–111.

Bakker, C.E., de Diego Otero, Y., Bontekoe, C., Raghoe, P., Luteijn, T., Hoogeveen, A.T., Oostra, B.A., and Willemsen, R. (2000). Immunocytochemical and biochemical characterization of FMRP, FXR1P, and FXR2P in the mouse. Exp. Cell Res. *258*, 162–170.

Barski, J.J., Dethleffsen, K., and Meyer, M. (2000). Cre recombinase expression in cerebellar Purkinje cells. Genesis *28*, 93–98.

Batchelor, A.M., and Garthwaite, J. (1997). Frequency detection and temporally dispersed synaptic signal association through a metabotropic glutamate receptor pathway. Nature *385*, 74–77.

Bravin, M., Morando, L., Vercelli, A., Rossi, F., and Strata, P. (1999). Control of spine formation by electrical activity in the adult rat cerebellum. Proc. Natl. Acad. Sci. USA *96*, 1704–1709.

Brown, V., Jin, P., Ceman, S., Darnell, J.C., O'Donnell, W.T., Tenenbaum, S.A., Jin, X., Feng, Y., Wilkinson, K.D., Keene, J.D., et al. (2001). Microarray identification of FMRP-associated brain mRNAs and altered mRNA translational profiles in fragile X syndrome. Cell *107*, 477–487.

Cesa, R., Morando, L., and Strata, P. (2003). Glutamate receptor delta2 subunit in activity-dependent heterologous synaptic competition. J. Neurosci. *23*, 2363–2370.

Chen, L., and Toth, M. (2001). Fragile X mice develop sensory hyperreactivity to auditory stimuli. Neuroscience *103*, 1043–1050.

Coesmans, M., Smitt, P.A., Linden, D.J., Shigemoto, R., Hirano, T., Yamakawa, Y., van Alphen, A.M., Luo, C., van der Geest, J.N., Kros,

J.M., et al. (2003). Mechanisms underlying cerebellar motor deficits due to mGluR1-autoantibodies. Ann. Neurol. *53*, 325–336.

Coesmans, M., Weber, J.T., De Zeeuw, C.I., and Hansel, C. (2004). Bidirectional parallel fiber plasticity in the cerebellum under climbing fiber control. Neuron *44*, 691–700.

Comery, T.A., Harris, J.B., Willems, P.J., Oostra, B.A., Irwin, S.A., Weiler, I.J., and Greenough, W.T. (1997). Abnormal dendritic spines in fragile X knockout mice: maturation and pruning deficits. Proc. Natl. Acad. Sci. USA *94*, 5401–5404.

De Vries, B.B., van den Ouweland, A.M., Mohkamsing, S., Duivenvoorden, H.J., Mol, E., Gelsema, K., van Rijn, M., Halley, D.J., Sandkuijl, L.A., Oostra, B.A., et al. (1997). Screening and diagnosis for the fragile X syndrome among the mentally retarded: an epidemiological and psychological survey. Collaborative Fragile X Study Group. Am. J. Hum. Genet. *61*, 660–667.

De Zeeuw, C.I., Holstege, J.C., Ruigrok, T.J., and Voogd, J. (1989). Ultrastructural study of the GABAergic, cerebellar, and mesodiencephalic innervation of the cat medial accessory olive: anterograde tracing combined with immunocytochemistry. J. Comp. Neurol. *284*, 12–35.

De Zeeuw, C.I., Hansel, C., Bian, F., Koekkoek, S.K., van Alphen, A.M., Linden, D.J., and Oberdick, J. (1998). Expression of a protein kinase C inhibitor in Purkinje cells blocks cerebellar LTD and adaptation of the vestibulo-ocular reflex. Neuron *20*, 495–508.

De Zeeuw, C.I., Elgersma, Y., Hulscher, H.C., Dortland, B.R., Hensbroek, R.A., Ruigrok, T.J., and Koekkoek, S.K.E. (2004). Response to comment on "Cerebellar LTD and Learning-Dependent Timing of Conditioned Eyelid Responses". Science *304*, 211C.

D'Hooge, R., Nagels, G., Franck, F., Bakker, C.E., Reyniers, E., Storm, K., Kooy, R.F., Oostra, B.A., Willems, P.J., and De Deyn, P.P. (1997). Mildly impaired water maze performance in male Fmr1 knockout mice. Neuroscience *76*, 367–376.

Dobkin, C., Rabe, A., Dumas, R., El Idrissi, A., Haubenstock, H., and Brown, W.T. (2000). Fmr1 knockout mouse has a distinctive strain-specific learning impairment. Neuroscience *100*, 423–429.

Fu, Y.H., Kuhl, D.P., Pizzuti, A., Pieretti, M., Sutcliffe, J.S., Richards, S., Verkerk, A.J., Holden, J.J., Fenwick, R.G., Jr., Warren, S.T., et al. (1991). Variation of the CGG repeat at the fragile X site results in genetic instability: resolution of the Sherman paradox. Cell *67*, 1047–1058.

Gruart, A., Pastor, A.M., Armengol, J.A., and Delgado-Garcia, J.M. (1997). Involvement of cerebellar cortex and nuclei in the genesis and control of unconditioned and conditioned eyelid motor responses. Prog. Brain Res. *114*, 511–528.

Gu, Y., McIlwain, K.L., Weeber, E.J., Yamagata, T., Xu, B., Antalffy, B.A., Reyes, C., Yuva-Paylor, L., Armstrong, D., Zoghbi, H., et al. (2002). Impaired conditioned fear and enhanced long-term potentiation in Fmr2 knock-out mice. J. Neurosci. *22*, 2753–2763.

Haasdijk, E.D., Vlug, A., Mulder, M.T., and Jaarsma, D. (2002). Increased apolipoprotein E expression correlates with the onset of neuronal degeneration in the spinal cord of G93A–SOD1 mice. Neurosci. Lett. *335*, 29–33.

Hagerman, R.J., and Hagerman, P.J. (2002). The fragile X premutation: into the phenotypic fold. Curr. Opin. Genet. Dev. *12*, 278–283.

Hinton, V.J., Brown, W.T., Wisniewski, K., and Rudelli, R.D. (1991). Analysis of neocortex in three males with the fragile X syndrome. Am. J. Med. Genet. *41*, 289–294.

Huber, K.M., Gallagher, S.M., Warren, S.T., and Bear, M.F. (2002). Altered synaptic plasticity in a mouse model of fragile X mental retardation. Proc. Natl. Acad. Sci. USA *99*, 7746–7750.

Ichikawa, R., Miyazaki, T., Kano, M., Hashikawa, T., Tatsumi, H., Sakimura, K., Mishina, M., Inoue, Y., and Watanabe, M. (2002). Distal extension of climbing fiber territory and multiple innervation caused by aberrant wiring to adjacent spiny branchlets in cerebellar Purkinje cells lacking glutamate receptor delta 2. J. Neurosci. *22*, 8487–8503.

Irwin, S.A., Patel, B., Idupulapati, M., Harris, J.B., Crisostomo, R.A., Larsen, B.P., Kooy, F., Willems, P.J., Cras, P., Kozlowski, P.B., et al. (2001). Abnormal dendritic spine characteristics in the temporal

and visual cortices of patients with fragile-X syndrome: a quantitative examination. Am. J. Med. Genet. *98*, 161–167.

Irwin, S.A., Idupulapati, M., Gilbert, M.E., Harris, J.B., Chakravarti, A.B., Rogers, E.J., Crisostomo, R.A., Larsen, B.P., Mehta, A., Alcantara, C.J., et al. (2002). Dendritic spine and dendritic field characteristics of layer V pyramidal neurons in the visual cortex of fragile-X knockout mice. Am. J. Med. Genet. *111*, 140–146.

Kakizawa, S., Yamasaki, M., Watanabe, M., and Kano, M. (2000). Critical period for activity-dependent synapse elimination in developing cerebellum. J. Neurosci. *20*, 4954–4961.

Kano, M., Hashimoto, K., Watanabe, M., Kurihara, H., Offermanns, S., Jiang, H., Wu, Y., Jun, K., Shin, H.S., Inoue, Y., et al. (1998). Phospholipase cbeta4 is specifically involved in climbing fiber synapse elimination in the developing cerebellum. Proc. Natl. Acad. Sci. USA *95*, 15724–15729.

Karachot, L., Shirai, Y., Vigot, R., Yamamori, T., and Ito, M. (2001). Induction of long-term depression in cerebellar Purkinje cells requires a rapidly turned over protein. J. Neurophysiol. *86*, 280–289.

Kelly, R.M., and Strick, P.L. (2003). Cerebellar loops with motor cortex and prefrontal cortex of a nonhuman primate. J. Neurosci. *23*, 8432–8444.

Kenyon, G.T., Medina, J.F., and Mauk, M.D. (1998). A mathematical model of the cerebellar-olivary system I: self-regulating equilibrium of climbing fiber activity. J. Comput. Neurosci. *5*, 17–33.

Kim, J.J., and Thompson, R.F. (1997). Cerebellar circuits and synaptic mechanisms involved in classical eyeblink conditioning. Trends Neurosci. *20*, 177–181.

Kim, S.G., Ugurbil, K., and Strick, P.L. (1994). Activation of a cerebellar output nucleus during cognitive processing. Science *265*, 949–951.

Koekkoek, S.K.E., Den Ouden, W.L., Perry, G., Highstein, S.M., and De Zeeuw, C.I. (2002). Monitoring kinetic and frequency-domain properties of eyelid responses in mice with magnetic distance measurement technique. J. Neurophysiol. *88*, 2124–2133.

Koekkoek, S.K., Hulscher, H.C., Dortland, B.R., Hensbroek, R.A., Elgersma, Y., Ruigrok, T.J., and De Zeeuw, C.I. (2003). Cerebellar LTD and learning-dependent timing of conditioned eyelid responses. Science *301*, 1736–1739.

Laggerbauer, B., Ostareck, D., Keidel, E.M., Ostareck-Lederer, A., and Fischer, U. (2001). Evidence that fragile X mental retardation protein is a negative regulator of translation. Hum. Mol. Genet. *10*, 329–338.

Leiner, H.C., Leiner, A.L., and Dow, R.S. (1993). Cognitive and language functions of the human cerebellum. Trends Neurosci. *16*, 444–447.

Li, Z., Zhang, Y., Ku, L., Wilkinson, K.D., Warren, S.T., and Feng, Y. (2001). The fragile X mental retardation protein inhibits translation via interacting with mRNA. Nucleic Acids Res. *29*, 2276–2283.

Linden, D.J. (2001). The expression of cerebellar LTD in culture is not associated with changes in AMPA-receptor kinetics, agonist affinity, or unitary conductance. Proc. Natl. Acad. Sci. USA *98*, 14066–14071.

Llano, I., Marty, A., Armstrong, C.M., and Konnerth, A. (1991). Synaptic- and agonist-induced excitatory currents of Purkinje cells in rat cerebellar slices. J. Physiol. *434*, 183–213.

Mauk, M.D., and Donegan, N.H. (1997). A model of Pavlovian eyelid conditioning based on the synaptic organization of the cerebellum. Learn. Mem. *4*, 130–158.

Medina, J.F., and Mauk, M.D. (2000). Computer simulation of cerebellar information processing. Nat. Neurosci. *3 (Suppl.)*, 1205–1211.

Middleton, F.A., and Strick, P.L. (1994). Anatomical evidence for cerebellar and basal ganglia involvement in higher cognitive function. Science *266*, 458–461.

Migaud, M., Charlesworth, P., Dempster, M., Webster, L.C., Watabe, A.M., Makhinson, M., He, Y., Ramsay, M.F., Morris, R.G., Morrison, J.H., et al. (1998). Enhanced long-term potentiation and impaired learning in mice with mutant postsynaptic density-95 protein. Nature *396*, 433–439.

Miyashiro, K.Y., Beckel-Mitchener, A., Purk, T.P., Becker, K.G., Bar-

ret, T., Liu, L., Carbonetto, S., Weiler, I.J., Greenough, W.T., and Eberwine, J. (2003). RNA cargoes associating with FMRP reveal deficits in cellular functioning in Fmr1 null mice. Neuron 37, 417–431.

Miyata, M., Okada, D., Hashimoto, K., Kano, M., and Ito, M. (1999). Corticotropin-releasing factor plays a permissive role in cerebellar long-term depression. Neuron 22, 763–775.

Nielsen, D.M., Derber, W.J., McClellan, D.A., and Crnic, L.S. (2002). Alterations in the auditory startle response in Fmr1 targeted mutant mouse models of fragile X syndrome. Brain Res. 927, 8–17.

Paradee, W., Melikian, H.E., Rasmussen, D.L., Kenneson, A., Conn, P.J., and Warren, S.T. (1999). Fragile X mouse: strain effects of knockout phenotype and evidence suggesting deficient amygdala function. Neuroscience 94, 185–192.

Rudelli, R.D., Brown, W.T., Wisniewski, K., Jenkins, E.C., Laure-Kamionowska, M., Connell, F., and Wisniewski, H.M. (1985). Adult fragile X syndrome. Clinico-neuropathologic findings. Acta Neuropathol. (Berl.) 67, 289–295.

Shibuki, K., Gomi, H., Chen, L., Bao, S., Kim, J.J., Wakatsuki, H., Fujisaki, T., Fujimoto, K., Katoh, A., Ikeda, T., et al. (1996). Deficient cerebellar long-term depression, impaired eyeblink conditioning, and normal motor coordination in GFAP mutant mice. Neuron 16, 587–599.

Strata, P., Morando, L., Bravin, M., and Rossi, F. (2000). Dendritic spine density in Purkinje cells. Trends Neurosci. 23, 198–198.

Teune, T.M., van der Burg, J., van der Moer, J., Voogd, J., and Ruigrok, T.J. (2000). Topography of cerebellar nuclear projections to the brain stem in the rat. Prog. Brain Res. 124, 141–172.

The Dutch-Belgian Fragile X Consortium. (1994). Fmr1 knockout mice: A model to study fragile X mental retardation. Cell 78, 23–33.

Turner, G., Webb, T., Wake, S., and Robinson, H. (1996). Prevalence of fragile X syndrome. Am. J. Med. Genet. 64, 196–197.

Van Dam, D., D'Hooge, R., Hauben, E., Reyniers, E., Gantois, I., Bakker, C.E., Oostra, B.A., Kooy, R.F., and De Deyn, P.P. (2000). Spatial learning, contextual fear conditioning and conditioned emotional response in Fmr1 knockout mice. Behav. Brain Res. 117, 127–136.

Van Pelt, J., Uylings, H.B., Verwer, R.W., Pentney, R.J., and Woldenberg, M.J. (1992). Tree asymmetry–a sensitive and practical measure for binary topological trees. Bull. Math. Biol. 54, 759–784.

Verheij, C., Bakker, C.E., de Graaff, E., Keulemans, J., Willemsen, R., Verkerk, A.J., Galjaard, H., Reuser, A.J., Hoogeveen, A.T., and Oostra, B.A. (1993). Characterization and localization of the FMR-1 gene product associated with fragile X syndrome. Nature 363, 722–724.

Verkerk, A.J., Pieretti, M., Sutcliffe, J.S., Fu, Y.H., Kuhl, D.P., Pizzuti, A., Reiner, O., Richards, S., Victoria, M.F., Zhang, F.P., et al. (1991). Identification of a gene (FMR-1) containing a CGG repeat coincident with a breakpoint cluster region exhibiting length variation in fragile X syndrome. Cell 65, 905–914.

Vokaer, M., Bier, J.C., Elincx, S., Claes, T., Paquier, P., Goldman, S., Bartholome, E.J., and Pandolfo, M. (2002). The cerebellum may be directly involved in cognitive functions. Neurology 58, 967–970.

Wang, S.S., Denk, W., and Hausser, M. (2000). Coincidence detection in single dendritic spines mediated by calcium release. Nat. Neurosci. 2, 1266–1273.

Weiler, I.J., Irwin, S.A., Klintsova, A.Y., Spencer, C.M., Brazelton, A.D., Miyashiro, K., Comery, T.A., Patel, B., Eberwine, J., and Greenough, W.T. (1997). Fragile X mental retardation protein is translated near synapses in response to neurotransmitter activation. Proc. Natl. Acad. Sci. USA 94, 5395–5400.

Xia, J., Chung, H.J., Wihler, C., Huganir, R.L., and Linden, D.J. (2000). Cerebellar long-term depression requires PKC-regulated interactions between GluR2/3 and PDZ domain-containing proteins. Neuron 28, 499–510.

Yeo, C.H., and Hesslow, G. (1998). Cerebellum and conditioned reflexes. Trends Cogn. Sci. 2, 322–331.